Astron. Astrophys. 259, 711–719 (1992)

ASTRONOMY AND ASTROPHYSICS

MUSICOS: a fiber-fed spectrograph for multi-site observations*

J. Baudrand and T. Böhm

Département d'Astrophysique Extragalactique et de Cosmologie, Observatoire de Paris, Section de Meudon, F-92195 Meudon Principal Cedex, France

Received September 11, accepted December 2, 1991

Abstract. This paper describes a fiber fed echelle spectrograph designed and constructed at the Paris-Meudon Observatory. This instrument is dedicated to the MUSICOS project, whose purpose is to organize multisite continuous spectroscopic observations. The optical scheme is described in some detail, as well as the data reduction software. We give a review of the spectrograph main performances which were obtained during laboratory tests and in real observational conditions at the 2 m diameter telescope at Pic du Midi (France).

Key words: spectroscopy – instruments – data analysis

1. Introduction

Many scientific programs linked to stellar physics research require continuous spectroscopic monitoring over several days. Continuous monitoring is indeed necessary for the study of several classes of variable phenomena:

(a) Phenomena with time scales of the order of one to three days, such as the variability due to rotational modulation. In particular, this variability can be studied in detail to provide Doppler images of stellar surface structures. The study of such phenomena is usually linked with the problem of stellar activity. Because stellar magnetic activity increases with rotational rate, the most interesting targets for this type of study are fast rotators, with rotational periods typically in the range of one to three days. A convenient phase coverage is difficult to obtain without continuous observations.

(b) Transient phenomena, such as stellar flares. Because of the random occurrence of these phenomena, their observation requires the organization of "patrols", whose probability of success is far higher when continuous coverage is possible.

(c) Periodic phenomena with periods shorter than one day, but for which side lobes of the observation window must be avoided. The best example of this category is asteroseismology.

MUSICOS (for MUlti-SIte COntinuous Spectroscopy) is an international project whose goal is to facilitate continuous spectroscopic coverage of stars, using multi-site observations on telescopes of the 2 m class (Foing et al. 1988; Catala & Foing 1990; Foing & Catala 1990). In the early phases of the project, it was recognized that a large number of existing telescopes of the 2 m class, distributed around the world, were lacking the spectroscopic equipment necessary to deal with the scientific problems mentioned above. The most efficient solution, ensuring the maximum productivity of future spectroscopic multi-site campaigns, would be to equip these telescopes with a set of identical spectrographs with characteristics well suited to the scientific programs requiring multi-site observations (Felenbok 1988). The MUSICOS strategy was defined accordingly, and consists of two complementary points:

1. Organize multi-site, multi-wavelength campaigns with the existing instruments, and by using existing transportable fiber-fed spectrographs, such as ISIS (Felenbok & Guérin 1987) or ISISbis (Cuby et al. 1990), on some of the 2 m class telescopes without spectroscopic equipment.

2. Define, design, build, and qualify the prototype of a cheap spectrograph meeting the requirements of the scientific programs requiring multi-site observations.

3. Reproduce this spectrograph and install the copies on telescopes of the 2 m class around the world.

A first MUSICOS campaign was organized in December 1989, using telescopes equiped with adequate spectrographs, and for which the ISIS and ISISbis fiber-fed spectrographs were transported to Xinglong (China) and to Mauna Kea (Hawaii), respectively. A full report about this campaign, as well as preliminary scientific results, were presented at the second MUSICOS workshop in March 1990 (Catala & Foing 1990). This campaign showed unambiguously the enormous interest of multi-site spectroscopic observations, but also the difficulty of analyzing spectroscopic data originating from spectrographs with different characteristics. These results confirm that a unique, standardized spectrograph, as well as a standard data reduction procedure, should ultimately be used for such campaigns.

Following point No. 2 of the MUSICOS strategy, a prototype of spectrograph was built at the Paris-Meudon observatory. A preliminary description of this instrument was given in Baudrand & Catala (1990). Its characteristics, defined according to the needs of the scientific programs, are the following:

(a) Wide spectral coverage. Most of the programs necessitating a continuous time coverage also need the simultaneous observation of many spectral lines. With the MUSICOS spectrograph, the whole visible range, from 380 to 880 nm is covered in two exposures: one "blue" exposure from 380 to 540 nm, and one "red" exposure, from 540 to 880 nm. In order to provide this wide coverage, the spectrograph works in the cross-dispersed configuration.

(b) Resolving power of at least 30000. This resolving power can be considered as adequate for Doppler imaging of rapid rotators, and for asteroseismology of solar-type stars, which are the most demanding programs in terms of resolving power.

Send offprint requests to: J. Baudrand

* Based on observations collected with the "Bernard Lyot" Telescope at Pic du Midi, France.

(c) High spectral stability. This requirement imposes the use of a table-top spectrograph, and a fiber illumination of the collimator.

(d) Easy transportability. A table-top spectrograph meets this requirement.

(e) High throughput efficiency.

(f) Possibility of simultaneously recording two spectra per frame. This feature is necessary for two kinds of programs: (i) measurements of magnetic fields by the Zeeman-Doppler technique (e.g. Semel 1989; Donati et al. 1989), which requires the simultaneous observation of spectra in the two states of circular polarization; and (ii) the prospective program of asteroseismology of solar-type stars (Brown et al. 1991), which requires to record simultaneously the spectrum of the star, and that of a stable calibration source.

(g) Low cost, in order to ensure easy duplication of the prototype.

The present paper describes this instrument in some detail. Section 2 provides a detailed description of the design and realization of the instrument, with the problems encountered, and a justification of the adopted solutions. In Sect. 3, we give the results of the laboratory tests that were performed on the elements of the spectrograph, as well as on the whole instrument after assembly. Section 4 describes the data reduction software associated with this spectrograph, which was adapted from existing software, in order to match the specificity of the instrument. In Sect. 5, the test observations performed on the 2 m Bernard Lyot telescope at Pic du Midi are presented and discussed. Section 6 contains the conclusion of this work and prospects for the future use of this spectrograph in multi-site spectroscopic campaigns.

2. Design considerations and description of the optical layout

During the detailed engineering phase we were chiefly guided by a very simple philosophy which was to achieve an efficient echelle spectrograph at the lowest possible cost. With such a guideline a fiber optic fed solution was the natural choice.

Fiber coupling, as it is now well understood, will ultimately provide the best wavelength precision, by producing nearly invariant flux distribution and consequently eliminating most slit zonal errors (Heacox 1986; Ramsey et al. 1986). In addition to this paramount characteristic, the fiber solution offers the possibility of supporting the optical train with a simple commercial and consequently low price mechanical structure that can be left on the floor, conveniently insulated from the moving telescope.

After evaluating tests conducted on several available step index fibers, we finally adopted the Polymicro FHA 50/70/90 that demonstrated good transparency and showed little microbending induced beamspreading. We planned to use its 50 μm diameter core as a direct circular entrance slit and to make it work with an F/2.5 injection focal ratio. This aperture is sufficiently low to prevent any losses by light scattering into the fiber cladding, but is fast enough to match a comfortable 2″ image on the sky through a 2-m class telescope.

In order to fulfil the specifications we designed a special fiber mount presenting two such identical fibers at the spectrograph entrance with a 180 μm separation between their axes so that two interleaved spectra could be obtained on the same exposure. The optical layout of the spectrograph is shown in Fig. 1.

Light leaving the fiber is directed toward the 400 mm focal length collimator, a paraboloid mirror subtending a F/4 aperture cone. Under these conditions of unperfect aperture matching (F/4 vs. F/2,5), our measurements showed that we shall have to acknowledge here a photon loss of about 35%. It must be stressed here that this loss was a compromise we were compelled to adopt with regard to our financial constraint:

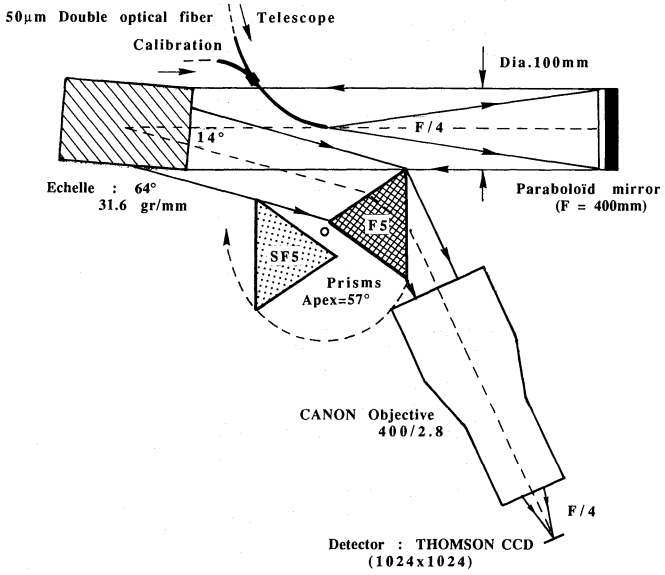

Fig. 1. Optical layout

In fact, as it is well known (see J. B. Hearnshow et al. 1986 for detailed comments and demonstration) the main design parameters of a fiber fed spectrograph are thoroughly defined once some of the instrumental characteristics and specifications of the project are declared (telescope diameter D, detector pixel size p, fiber core angular diameter at the telescope focal plane α and resolving power R).

For example, the numerical aperture of the camera optics O_3 can be straightforwardly derived from the relation

$$O_3 = O_2/O_1 \; \alpha D/(2.5\,p).$$

Where 2.5 pixels provides good sampling of the projected fiber core onto the detector and O_2/O_1 represents the beam degradation (due to the spreading of the output cone from the fiber) with O_2 and O_1 the aperture of the light cone at the fiber output and input respectively.

In concrete terms in our case, the conditions specified by the project ($D = 2$ m, $\alpha = 2''$, $p = 19$ μm) led to a $\approx$F/2.5 camera.

The fiber core diameter d, as well as the collimator focal length f, are linked to the resolving power by the formula

$$R = 2 \operatorname{tg}\beta \; f/d \quad \text{with } \beta \text{ the grating blaze angle.}$$

With the minimum 30 000 resolving power imposed by our specifications and the highest blaze angle of the readily available commercial gratings ($\operatorname{tg}\beta = 2$) we then have:

$$f/d \geqq 7500$$

and any couple of values respecting this ratio will be acceptable (but one would be advised to keep d as low as possible in order to work with fast input conditions on the fiber and consequently take advantage of a negligeable focal ratio degradation).

Now, the collimated beam size is another very important parameter of the design since the dimensions of the grating (an expensive piece of equipment) is directly dependent on it. The

diameter B of this beam is also perfectly set by our initial conditions and it can be easily demonstrated that:

$B = f/d\ O_3\ 2.5p$ which in our case gives $B \geqq 150$ mm.

Thus, we can see that with the specifications we were given, the optimum solution would have required at the same time, a fast camera and a large echelle grating. This was unfortunately beyond our financial possibilities and we were therefore compelled to apply some degradation on the design. Since the MUSICOS scientific programs prohibited any relaxation on the spectral characteristics (resolving power and spectral coverage) the only possibility was to lose some of the incident light somewhere. As it was described above, we chose to lose it at the fiber output end, with a F/4 collimator, rather than at the input by reducing the focal plane scale, mainly because the instrument could very possibly be used on poor quality sites during the MUSICOS campaigns and that the latter scheme could always be easily adopted under good seeing conditions in order to yield better collecting performances.

It is also worth mentioning here, that the attractive solution to use a fiber with a larger core diameter associated with an image slicer was also discarded because of the resultant broadening and awkward overlapping of the echelle orders on the limited format (20 mm × 20 mm) of the CCD detector selected for the project.

Following the 100 mm diameter collimated beam, we come now to the echelle grating, a Milton Roy replica (31.6 gr/mm and 63°5 blaze angle) which was, as we said above, certainly the best choice among the available gratings to ensure high resolving power and convenient short free spectral range for good wavelength coverage with small aperture detectors (Schroeder 1967).

It is illuminated under Littrow conditions, for best blaze efficiency, and with a small 7° conical imaging, necessary to clear away the refracted light towards our second perpendicular dispersing element: a prism used in single pass mode, more appropriate than a grating for throughput efficiency as well as for order compacting considerations (Schroeder 1970).

However, it was necessary to select two different glass materials, F 5 and SF 5, from the SCHOTT company, so as to meet the distinct dispersion requirements of the two wavelength regions, 380–540 nm and 540–880 nm respectively (hereinafter referred as blue and red regions for the sake of simplicity).

The beam emerging from the prism with an average total deviation of 60° is then projected onto the detector by means of a 400/2.8 CANON objective, giving an overall spectrograph magnification of 1.

This simple optical disposition along with the choice of the appropriate camera optics was a crucial aspect of our design: On the one hand, because of the redistributed pupil of our design (resulting from light scrambling within the fiber) it was no longer possible to make use of the telescope secondary shadow and accordingly, a folded Schmidt-camera scheme, with its central vignetting was rejected. On the other hand, a convenient Czerny-Turner configuration (where coma and distortion are eliminated while room is provided for the detector without obscuration) would have produced spherical aberration and astigmatism that should have been accounted for and corrected, either in a reconstructed pupil or by the camera itself. This solution was also rejected for the same economical reason that was evocated before, as well as for spectral stability considerations (a vital aspect of our project) since the long optical train of the Czerny-Turner arrangement would have been extremely sensible to mechanical flexure.

Thus, we ultimately studied this short in line solution, whose dioptric camera, considering our context, was to be sought among available commercial objectives quite cheap when compared with special computed optics (nearly ten times as expensive).

The drawback with this strategy lies in the impossibility of making accurate predictions with regard to photometric efficiency and achromatism, especially over a wavelength range greatly exceeding the manufacturer's specifications. So our only alternative was to set up a comparative laboratory trial with the three possible commercial candidates that were kindly lent by the CANON, NIKON and OLYMPUS companies respectively. After time consuming tests it was eventually demonstrated that the CANON element exhibited the best performance and could be adapted to our requirements (see Appendix A for comparative tests).

Because of the two distinct cross-dispersers and of the residual chromatism of the CANON objective, the alternating passage from the blue to red spectral regions imposed 4 independent mechanical drives:

(a) 180° rotation of the prism platform for intercepting the beam with the appropriate element.

(b) 5° shift of the structure supporting both objective and detector camera in order to align them with the two distinct blue and red prism deviations.

(c) Small but necessary translation and tilt of the detector with respect to the camera objective to match its blue and red distinct focal planes.

All these motions are motorized and simultaneously commanded. They require less than three minutes for the color shift and yield an optical positioning precision lying within one 19 μm CCD pixel.

Finally, with this simple optical arrangement where elements are located very close to each other, we have obtained an extremely efficient and compact train that can be fitted comfortably on a small 1.5 square meter optical table.

From our local French experience, we estimate that this spectrograph could be duplicated with a moderate budget of 40 000 U.S. dollars budget (workshop mechanics included) and within a short 6 month delay, as most of the elements are readily available and can be conveniently purchased from well established firms (see Appendix B for a summary of the spectrograph main parameters).

3. Laboratory results

3.1. Throughput optical efficiency

Particular attention was given to the energy throughput quality of our instrument.

As we said earlier we designed a solution with no vignetting of the beam anywhere along the optical path (except for the negligible shadow of the fiber itself at spectrograph entrance).

The echelle grating is used under Littrow condition to ensure the best blaze efficiency and the prism faces are treated with optimized multi-layer broad band antireflection coatings.

As for the fiber and the camera objective, they were selected to give the best transparency, especially in the blue.

We performed careful measurements on each element of the optical chain, and a direct overall photometric evaluation, between the fiber input face and the camera objective focal plane, confirmed the individual results, with a 17% throughput efficiency. This value was found at blaze center and over most of our spectral coverage. It is clear however that the speed of the instrument can be significantly degraded, especially in the bluest

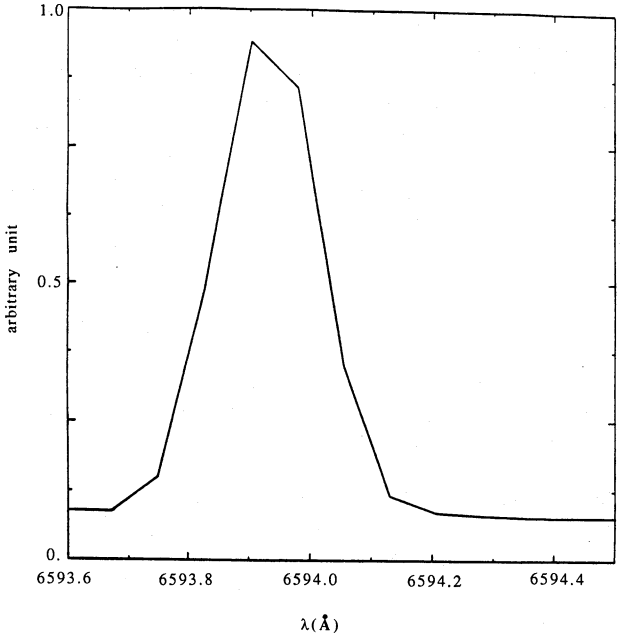

Fig. 2. Instrumental profile. Unresolved emission line from a thorium lamp ($\lambda = 6593.939$ Å) yielding a resolving power $R = 36000$

part of our spectral range (because of the reduced transparency of the fiber and quantum efficiency of the CCD detector) and at the edge of the detector format, far from the blaze function maximum.

3.2. *Instrumental profile*

Taking into account the total aberration of the system (astigmatism, coma and spherical aberration), the circular 50 μm slit is projected along the main dispersion direction onto 2.5 pxl of our current Thomson CCD. These optimum sampling conditions are respected over the entire 1024 × 1024 CCD frame, owing to the good matching of the detector surface with the camera focal plane.

Figure 2 shows a recorded unresolved thorium line. The profiles of the thorium lines proved to be symmetric and have a measured half-intensity width that fulfils our expectations, yielding a resolving power between 35000 and 40000 (we obtained this result on a sample of about 50 emission lines well distributed over the whole λ-domain).

3.3. *Layout and separation of the orders*

With the two selected prisms, it was possible to fan out the successive echelle orders with the optimum dispersion, allowing the stacking of 2 × 40 orders per CCD exposure with just the necessary gap to prevent unwanted overlapping. Figure 3 presents typical blue and red exposures with two interleaved spectra, a continuum from a Tungsten lamp and a wavelength calibration spectrum from a neon-thorium source.

Through the recorded intensities, we can easily notice the strong effect of the blaze function, whose maximum is perfectly situated at the center of the CCD frame. As was expected from the single slit diffraction pattern, intensities at the ends of each order are approximately 40% of those at blaze peak.

Other features can be noticed: one is the slight curvature of the orders, and the other is the ovalization of the spectral lines and their resultant apparent slant with respect to the grating dispersion. The prism cross disperser anamorphose and the 7° conical

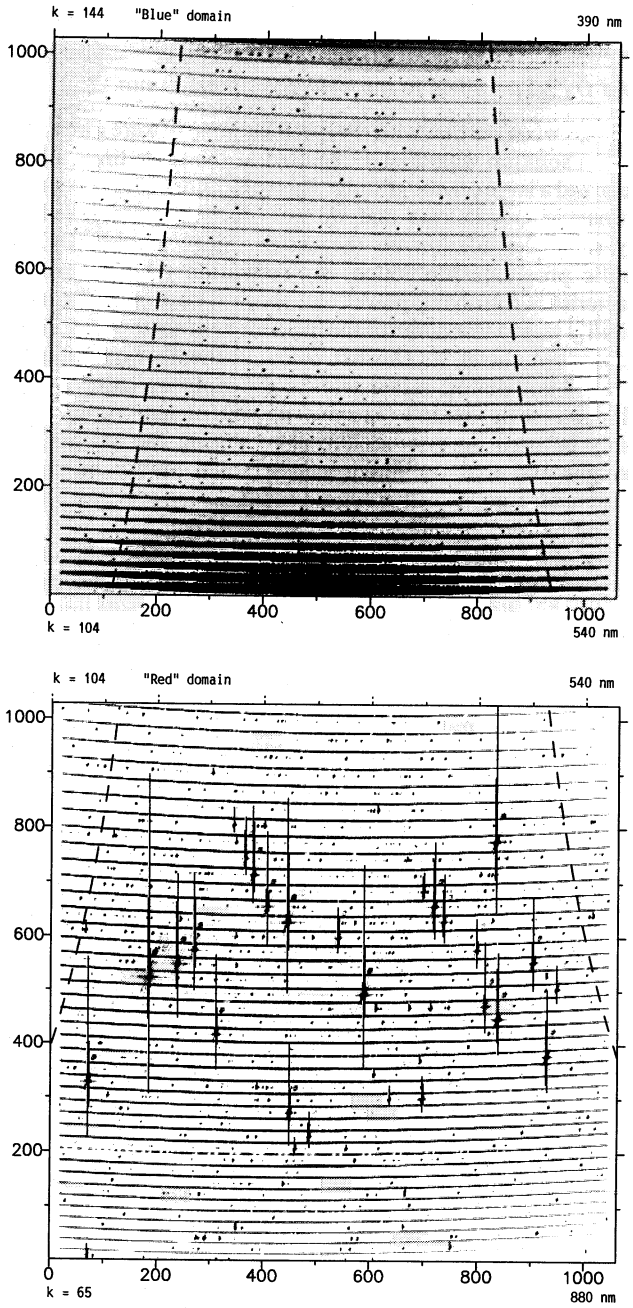

Fig. 3. Echellograms. Typical "blue" and "red" exposures on a THOMSON CCD 1024 × 1024, with two interleaved spectra: a continuum from a tungsten lamp and a wavelength calibration spectrum from a Th/Ne lamp (the free spectral range is represented by the dashed lines)

incidence on the echelle are mainly responsible for this situation (Marechal 1952), which however presents no particular problem, neither for the order extraction nor for the ultimate spectral resolution, as will be explained later in the data reduction section.

We have also represented, for clarity, the echelle cycle length (the linear distance between the same wavelength in adjacent orders) which increases rapidly towards the longer wavelengths, according to the echelle theory. As can be seen, the spectral coverage is complete until the 80th order ($\lambda = 700$ nm) where the echellogram is trunkated by the CCD frame. This limitation, due to the moderate size of the detector (Thomson 1024 × 1024), is not

an important drawback since most of the lines of astrophysical importance (with one exception: Ca II 846.2 nm) are included into the format.

The minimum separation between two adjacent orders at the longer wavelength side of each exposure is 360 μm and less than twice this value at the opposite side. With a 180 μm interval between the axes of the twin fibers, it leaves just enough room for clean photometric separation of the two companion spectra.

4. Data reduction software

In this section we describe the automatic procedure to reduce MUSICOS echelle spectra. Based on the ECHFIC program, developed by Monique Spite (Spite 1990) for different echelle spectrum reductions (CASPEC, ECHELEC,...) we produced a specially adapted version named MUSBIC taking into account the rather different instrumental specifications. It works for any 1024 × 1024 CCD. As the acquisition, the reduction is divided into two spectral domains: the red domain (550–890 nm) and the blue domain (390–550 nm). Both domains are precisely defined with regard to the order positions. The orders of MUSICOS are rather curved (maximum curvature about 13 pxl). The approximate position of each order is given at 3 points (pixel coordinates) and read in two tables (one for each domain). These positions do not vary significantly during an observing run, but can differ from one run to another. Therefore the approximate order positions are recomputed once for each run using a sufficiently exposed red and blue flatfield exposure by an auxiliary program (MUSADJUST). However, if instrumental adjustments are done with enough precision (after each transport of the instrument) even this preliminary work is unnecessary.

In order to determine the exact position of an order the program adjusts a parabola through the 3 corresponding points read in the table. Then it defines 10 equally spaced columns (perpendicular to the order) over the whole CCD width. In these columns the program extracts a 12 pxl high slice around the previously fitted positions. The centroïd of the order is carefully determined inside each slice, then a 5th degree polynomial is fitted through the 10 centroïd positions. This high degree is necessary to take into account the non symmetric curvature of the orders. This procedure can be performed either on the object spectrum (if sufficiently exposed), or on another stellar or flatfield spectrum obtained with the same setup of the spectrograph. The result is an accurate position for each order appearing on the spectrum.

In a second step, the program extracts each order of the object spectrum and of the auxiliary spectra (flatfield, thorium) around the positions determined in the first step. The half-widths of the nearly Gaussian order profile (perpendicular to the dispersion) vary between 2.5 and 3.5 pxl for the blue and for the red domain, respectively. Therefore the extraction width (around the centroïd) is usually 7 pxl for the blue domain and 9 pxl for the red one, so that it contains most of the signal.

In the third step we integrate the extracted signal above the baseline defined by the mean value of the signal at the adjacent interorder positions.

Centroïds of the orders of different spectra were shown to differ by less than 0.1 pxl owing to fiber-feeding. This makes a flatfield calibration possible which maintains the SNR as high as possible: in this case it is indeed mathematically rigourous to integrate the stellar and flatfield signal perpendicularly to the dispersion (along the columns) before dividing the stellar spectrum by the flatfield spectrum.

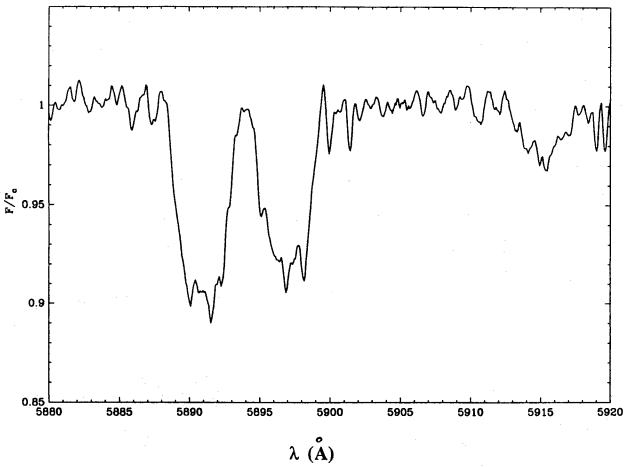

Fig. 4. Software-reduced spectrum. Totally reduced spectrum in the region of the Na I lines ($\lambda = 5889.973$ Å and $\lambda = 5895.949$ Å) from HD 84999. Notice that this spectrum has been smoothed with a sliding mean of 2 pxl (while the resolved element has a width of 2.2 pxl)

Two data tables contain wavelengths and pixel positions of all significant emission lines for each order of a thorium reference spectrum (up to 20 per order). Usually, these pixel positions (in the dispersion direction) do not differ much between two observational runs. In the worst case one wavelength/pixel position for each domain must be entered in order to allow the program to take into account a possible shift. Starting from guessed positions read in the tables, the program finds by itself the exact positions and automatically deduces for each order the coefficients of the 3rd order polynomial giving the wavelength calibration λ(pxl).

In Fig. 4, we show an example of a totally reduced spectral domain around the Na I lines ($\lambda = 5889.973$ Å and $\lambda = 5895.949$ Å).

Finally, the output file of MUSBIC can be converted by an auxiliary program into eVe-standard (Bijaoui et al. 1986) or into other formats readable by large software package (like MIDAS, IRAF,...). The program is transportable between UNIX and VMS and this version needs not more than 3.5 min of CPU on a VAX 3200 station to reduce a whole λ-domain. To use MUSICOS in its 2 fiber configuration for ultraprecise radial velocity monitoring and spectropolarimetry, which require the simultaneous observation of 2 spectra with interleaved orders, a special two fiber version of MUSBIC is being developed. The total reduction procedure will also be automatic. Order concatenation in the dispersion direction (end to end assembling of the spectrum constituting orders) and automatic continuum normalisation procedures are also being installed.

5. Astronomical observations at the Pic du Midi Observatory

5.1. *Set up of the experiment*

To complete the spectrograph qualification it was of course necessary to evaluate its performances under real observational conditions, behind a 2 m class telescope. This phase was performed during the 1991 winter on the Bernard Lyot telescope at Pic du Midi, France.

During these experimental runs, our instrument was safely installed in a small dark room at the telescope control level and optically linked to the cassegrain focus with a 20-m

POLYMICRO fiber. The mechanical coupling was realized through a Cassegrain adaptor, a small closed structure, incorporating the usual essential functions:

(a) Focal reduction to size the stellar image to the fiber core (Passage from F/25 to F/2.5 by means of a high quality cemented glass achromat).

(b) Stellar guiding on the fiber through a reimaging system, a sideway holed reflector facing a small CCD camera.

(c) Presentation to the spectrograph of suitable calibrations with lamps, sources and matching optics.

As we wanted to simulate radial velocity monitoring, the input end of the second fiber was connected to a static optical arm bench in order to give the necessary wavelength reference.

All our spectra were recorded with the station acquisition system and its cooled camera device incorporating a 1024×1024 CCD THOMSON which was front side illuminated and enhanced in the blue with appropriate coating (Metachrome II). The camera was found to be linear up to $2\ 10^5$ e pxl^{-1} and its read out noise was measured at 15 e pxl^{-1}.

5.2. *Speed of the instrument*

Relying upon the reduction of the observational data accumulated during good atmospheric conditions (seeing $\approx 1''$), it is now possible to give a relevant evaluation of the speed of the spectrograph, including the CCD detector.

While photon limited, a one hour time exposure with a 2 m telescope on a $m_v = 7$ A0V star will yield at the blaze center the S/N ratios indicated in the table below (quantum efficiencies of the CCD are also given for each wavelength). These values are estimated from results obtained on stars of different spectral classes and magnitudes and they are given per spectral resolved element spread on 2.5 CCD pxl, which in this case yields a 34000 resolving power. (Note the low Q.E at 400 nm of the CCD we used for these tests. A thinned CCD would yield much better results at this wavelength.)

λ (nm)	S/N	CCD Q.E (%)
400	125	12
500	320	30
600	405	45
700	380	40
800	300	30

5.3. *Resolving power*

The resolving power of the instrument has been determined to vary around $R = 38000$ (rms 3000) across the CCD, which is a better value than expected.

5.4. *Wavelength stability*

Brown et al. (1991) showed that a cross-dispersion spectrograph recording a wide spectral domain may be an efficient solution for detecting and measuring pulsations in solar-type stars. The method of Brown et al. (1991) consists of recording simultaneously the stellar spectrum and that of a stable reference (like a hollow cathode Th/Ar lamp).

The MUSICOS spectrograph has the desired characteristics to perform this type of observations, but careful checks concerning its ultimate stability must be performed before adapting it for use in asteroseismologic observations.

Measurements of wavelength stabilities were made on raw non extracted or treated spectra, to avoid the introduction of a kind of "software reduction noise". To test this stability, we simultaneously took spectra on both fibers by using the two fiber set-up of our instrument: the first fiber collected the flux of a cool, slowly rotating G8III star (HD 113226) with many narrow photospheric absorption lines and the second one took a comparison Th/Ne spectrum. First statistics were made on a sample of 9 spectra, spanning a total time of one hour.

In order to determine emission or absorption line centroïds we extracted one pixel large slices of the CCD image, crossing well chosen lines: the absorption lines of the star we used for measurements had to show a single, non-blended line profile; the Th/Ne emission lines had to be sufficiently exposed to ensure a good Gaussian fitting. Left and right limitations of the fittings were taken identically for all measurements on the whole sample.

In a first step we wanted to analyse global stability evolution. We noted on this sample of images a maximum line centroïd difference (in the dispersion direction of 0.15 pxl (rms: 0.04 pxl). Perpendicular to this direction the stability was even higher (maximum order centroïd difference: 0.06 pxl).

On a higher level of investigations we analyzed relative stability (with regard to the calibration spectrum) in order to correct for instability induced by instrumental motions. By using a high number of emission and absorption lines we noticed the following stability characteristics:

(a) rms of differential stability is lower than 0.025 pxl.

(b) small instabilities (inside the rms) are generally non-correlated (no global motion between star and reference spectra is apparent at this level of precision).

With a resolving power around $R = 35000$, a stability of 0.025 pxl, and assuming a sample of 400 non-correlated measured pairs of lines on each spectrum and the total amount of 2000 spectra taken during a whole observational week (2 min for each spectrum) we could obtain a radial velocity noise of about 10 cm s^{-1}, in the absence of any systematic effect not yet experienced with this spectrograph.

These results indicate that the use of such a spectrograph can be envisaged for future observations of pulsations of solar-type stars, with a method similar to that of Brown et al. (1991).

5.5. *Scattered light*

The determination of scattered light is a very difficult problem in an echelle spectrograph. We have to consider a superposition of the global scattered light perpendicular to the dispersion, the traditionally named "scattered light" parallel to the dispersion from the adjacent continuum, the overlapping of the instrumental profile of adjacent orders and thermal "dark" noise.

Even if we are unable to give "one" scattering coefficient due to the complexity of the situation, we can present some general observations.

The inter-order minima are approximately 3% of the adjacent order peak intensities. Note that McCarthy (1990) obtained the same result for the Palomar 1.5 m echelle spectrograph. By subtraction of a mean value of the adjacent inter-order minima we obtain, after total reduction, the following regression line for equivalent widths (W_λ) measured on a lunar spectrum and compared to the atlas from Moore et al. (1966):

$$W_\lambda(\text{atlas}) = 0.98\ W'_\lambda(\text{MUSICOS}) - 3.85\ (\text{mÅ}).$$

Burnage & Gerbaldi (1990) obtain with the same method of background subtraction almost the same regression line on spectra from the ECHELEC spectrograph on the 1.5 m ESO telescope.

We therefore conclude that the behaviour of MUSICOS with regard to scattered light is inside the norms. Analytical modelling of the scattered light is very difficult. Profiles and absorption features of adjacent orders play an important role in regard to scattered light, but are difficult to take into account in an analytical code (Appendix C). The calculations in Appendix C show that the coefficients of the regression line here-above can be identified with average values of analytical terms.

The best way to subtract background light (including electronic offset, dark current, scattered light, ...) is being investigated. Possibilities are subtraction of a constant dark noise value, subtraction of the mean value at adjacent interorders (used at this moment) or the use of a more empirical, but more precise method as suggested by Gehren & Ponz (1986).

6. Conclusion

In this paper, we have presented the prototype of a fiber-fed cross-dispersed echelle spectrograph, meant to be duplicated and used during multi-site spectroscopic MUSICOS campaigns. This spectrograph provides a spectral coverage of the visible domain from 380 to 880 nm in two exposures, with a resolving power ranging from 35000 to 40000. Its spectral stability, i.e. the rms motion of the spectra on the CCD in the direction of the dispersion, amounts to about 0.04 pxl, corresponding to 0.16 km s^{-1}. When a thorium lamp spectrum is recorded simultaneously with the stellar spectrum, most of the systematic motions of the instrument can be corrected, and the spectral stability drops down below 0.025 pxl, corresponding to 0.1 km s^{-1}. This high stability indicates that the MUSICOS spectrograph can be considered as a potential instrument for future observations of oscillations of solar-type stars. The throughput of the instrument corresponds to the expected performances, to within a factor of 3, which we attribute mainly to the atmospheric conditions during the test observations, and also possibly to the mechanical centering of the fiber at the telescope focus. Work is presently under way to improve this centering. The present performances of the spectrograph are such that a S/N ratio of 350 per resolved element can be reached in 1 h on a 7th magnitude A0 star at 550 nm.

The MUSICOS spectrograph will be operated routinely on the 2 m Bernard Lyot telescope at the Pic du Midi Observatory, starting in 1992. It will also be transported to remote sites for future multisite spectroscopic MUSICOS campaigns. Such a campaign is presently in preparation, and should be carried out in Dec. 1992. We envisage transporting the MUSICOS spectrograph to the University of Hawaii 2 m telescope, if observing time is allocated to us on this telescope for this campaign.

The laboratory and astronomical tests of the MUSICOS spectrograph show that it meets perfectly the needs of the scientific stellar programs requiring multi-site spectroscopic observations. Moreover, the cost of this spectrograph, excluding the detector, remains very low. It is therefore very easy to copy, and we are ready to provide all technical details to anyone who would be interested in its reproduction, If a sufficient number of copies of this spectrograph can be built and mounted on telescopes of the 2 m class well-distributed in longitude around the world, all the conditions will be met for organizing multi-site spectroscopic campaigns with a very high probability of success.

As the next stage in this effort to propose a standardized instrument for multi-site campaigns, we are currently designing a cheap CCD camera, based on a Thomson 1024 × 1024 chip, with (19 μm)^2 pxl. The cost of this camera should not exceed that of the spectrograph.

Acknowledgements. We want to thank all the people who have contributed to this work and especially Dr. Paul Felenbok for his crucial advice, Dr. Claude Catala for his deep involvement during the instrument qualification period, Monique Spite who has kindly given us access to her data reduction software, the staff of the Bernard Lyot telescope at the Pic du Midi for their kind and efficient support and Mr. Michel Lesserteur who designed the mechanical layout at the CNRS Meudon Bellevue Bureau d'Etudes des Prototypes. The realisation of the MUSICOS spectrograph was supported financially by the Institut National des Sciences de l'Univers (INSU, CNRS), which we gratefully acknowledge.

Appendix A: commercial objective test results

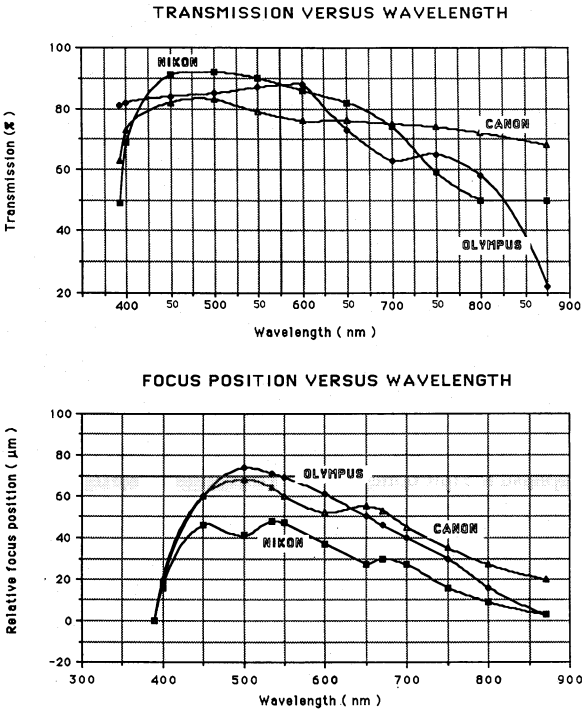

Fig. A1

Appendix B: summary of the echelle spectrograph parameters

Resolutions of about 35000 are achieved over a wavelength region ranging from 380 to 880 nm with throughput efficiency of 17% for light that enters into the fiber.

Fiber:	step index silica 50 μm diameter core (POLYMICRO)
Collimator:	on-axis paraboloïd mirror; $F = 400$ mm
Echelle grating:	MILTON-ROY 31.6 gr/mm blaze angle = incidence angle = 63°5 conical incidence = 7°
Cross disperser:	prisms, F5 and SF5 (SCHOTT) apical angle = 57° incidence angle = 45°
Camera:	CANON objective 400/2.8
Slit image at focal plane:	50 μm scaling 2″1 on the sky
Average order separation:	500 μm
Separation between interleaved spectra:	180 μm
Number of orders:	80 orders in two spectral domains

Appendic C: analytical modelling of scattering in an echelle spectrum with interorder background subtraction

The value subtracted from the integrated flux is the average of the interorder fluxes on both sides of the central order, themselves being smoothed in the direction of the dispersion by a 9 point sliding mean. The signal on each pixel of the CCD is a superposition of several components: object signal, background noise (dark current, readout noise), scattered light in the direction of the dispersion and in the direction perpendicular to the dispersion (flux coming from the wings of the adjacent orders). The scattered light coefficient usually given for a mono-order spectrograph isü the one concerning the direction of the dispersion (line filling by adjacent continuum). In the following analytical development we try to separate the scattering into two perpendicular contributions, in order to compare it with the result of a mono-order spectrum.

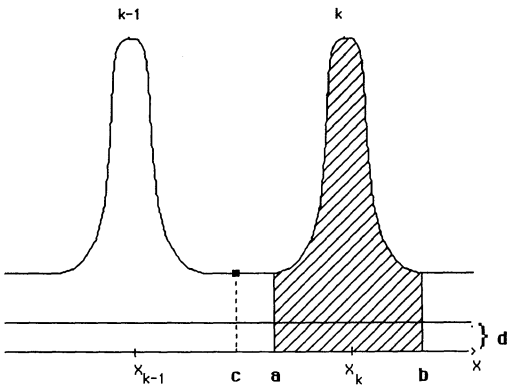

Fig. C1. Shows a section through two adjacent orders of an echell spectrum. Points a and b are the limits of integration of the flux perpendicular to the dispersion. Point c indicates the location where the interorder background (between orders k and $k-1$) is determined.

If the order k were isolated, the total signal at a given position along the order would be:

$$I(\lambda) = I_k(\lambda) = I^*(\lambda) + \varepsilon_d I_C$$

where I^* is flux from the object at wavelength λ, I_C is flux from the adjacent continuum of an absorption line, and ε_d is scattering coefficient in the dispersion direction.

All orders are assumed to have the same instrumental profile $G(x-x_k)$ perpendicular to the dispersion (for the sake of simplicity), where x_k is the center of the order k. We thus have

$$I_k(x) = I_k\, G(x-x_k) \quad \text{with} \quad \int G(x-x_k)\,\mathrm{d}x = 1.$$

The extracted signal S (at wavelength λ) is composed of the signal I integrated over a domain defined by a and b centered on the order centroïd, of the background noise d integrated between a and b, of the contribution from the wings of adjacent orders (depending on the fluxes of the adjacent orders: I_{k-1} and I_{k+1}) and corrected by subtracting the average of the interorder backgrounds between the orders $k-1$, k and k, $k+1$.

Defining position $c = \frac{1}{2}(x_k + x_{k-1})$ and $c' = \frac{1}{2}(x_{k+1} + x_k)$, we can write:

$$\begin{aligned} S = {} & \kappa\, I + d(b-a) + \phi(I_{k-1}, I_{k+1}) \\ & - \tfrac{1}{2}\,[d + G(c-x_{k-1})\, I_{k-1} + G(c-x_k)\, I_k + G(c-x_{k+1})\, I_{k+1} \\ & + d + G(c'-x_{k-1})\, I_{k-1} + G(c'-x_k)\, I_k \\ & + G(c'-x_{k+1})\, I_{k+1}]\,(b-a) \end{aligned}$$

where

$$\kappa = \int_a^b G(x-x_k)\,\mathrm{d}x$$

is a coefficient smaller than unity and where

$$\phi(I_{k-1}, I_{k+1}) = \int_a^b [G(x-x_{k-1})\, I_{k-1} + G(x-x_{k+1})\, I_{k+1}]\,\mathrm{d}x\,.$$

Assuming that the transverse order profiles are symmetric and that both adjacent orders are equidistant from the central order, we have:

$$\int_a^b G(x-x_{k-1})\,\mathrm{d}x = \int_a^b G(x-x_{k+1})\,\mathrm{d}x$$

We therefore obtain:

$$\phi(I_{k-1}, I_{k+1}) = (I_{k-1} + I_{k+1}) \int_a^b G(x-x_{k-1})\,\mathrm{d}x\,.$$

Defining $I_1 = I_{k-1} + I_{k+1}$ and $e_b = \int_a^b G(x-x_{k-1})\,\mathrm{d}x$

we can write: $\phi(I_{k-1}, I_{k+1}) = e_b I_1$.

We also define e_{c1} and e_c such that:

$$\begin{aligned} & G(c-x_{k-1}) + G(c'-x_{k-1}) \\ & \quad = G(c-x_{k+1}) + G(c'-x_{k+1}) = 2\frac{e_{c1}}{b-a} \end{aligned}$$

and $G(c-x_k) = G(c'-x_k) = \dfrac{e_c}{b-a}$.

We finally obtain

$$S = \alpha I + e'' I_1$$

with $\alpha = \kappa - e_c$ and $e'' = e_b - e_{c1}$

In this expression α is *smaller than unity* and our experience shows that e'' *is usually negative.*

Thus we obtain:

$$S(\lambda) = \alpha I^*(\lambda) + \alpha \varepsilon_d I_C + e'' I_1(\lambda)$$

and $S_C = S(\lambda = \lambda_C) = \alpha(1 + \varepsilon_d) I_C + e'' I_1(\lambda_C)$

with $I_C = I(\lambda = \lambda_C)$

$$\text{so } \frac{S}{S_C} = \frac{I^*\left[1 + \varepsilon_d \frac{I_C}{I^*} + \frac{e'' I_1}{\alpha I^*}\right]}{I_C\left[1 + \varepsilon_d + \frac{e'' I_1(\lambda_C)}{\alpha I_C}\right]}$$

$$= \frac{I^*}{I_C}\left[1 + \varepsilon_d \frac{I_C}{I^*} + \frac{e'' I_1}{\alpha I^*}\right]\left[1 - \varepsilon_d - \frac{e'' I_1(\lambda_C)}{\alpha I_C}\right] + \ldots$$

$$= \frac{I^*}{I_C}\left[1 + \varepsilon_d\left(\frac{I_C}{I^*} - 1\right) + \frac{e''}{\alpha}\left(\frac{I_1}{I^*} - \frac{I_1(\lambda_C)}{I_C}\right)\right] + \ldots$$

$$= \frac{I^*}{I_C} + \varepsilon_d - \varepsilon_d \frac{I^*}{I_C} + \frac{e'' I_1}{\alpha I_C} - \frac{e'' I_1(\lambda_C) I^*}{\alpha I_C^2} + \ldots .$$

We deduce the following expression for the equivalent width (W'_λ) measured for an absorption line (signal integrated between the adjacent continuum wavelengths (λ_0 and λ_1), as a function of the actual equivalent width W_λ:

$$W'_\lambda = \int_{\lambda_0}^{\lambda_1}\left(1 - \frac{S(\lambda)}{S_C}\right) d\lambda$$

$$= \int_{\lambda_0}^{\lambda_1}\left(1 - \frac{I^*(\lambda)}{I_C}\right) d\lambda - \varepsilon_d \int_{\lambda_0}^{\lambda_1}\left(1 - \frac{I^*(\lambda)}{I_C}\right) d\lambda$$

$$- \frac{e''}{\alpha}\int_{\lambda_0}^{\lambda_1}\left(\frac{I_1(\lambda)}{I_C} - \frac{I_1(\lambda_C) I^*(\lambda)}{I_C^2}\right) d\lambda$$

$$= (1 - \varepsilon_d) W_\lambda - \frac{e'' I_1(\lambda_C)}{\alpha I_C}\int_{\lambda_0}^{\lambda_1}\left(\frac{I_1(\lambda)}{I_1(\lambda_C)} - \frac{I^*(\lambda)}{I_C}\right) d\lambda$$

$$= (1 - \varepsilon_d) W_\lambda - \frac{e'' I_1(\lambda_C)}{\alpha I_C}$$

$$\cdot\left[\int_{\lambda_0}^{\lambda_1}\left(1 - \frac{I^*(\lambda)}{I_C}\right) d\lambda - \int_{\lambda_0}^{\lambda_1}\left(1 - \frac{I_1(\lambda)}{I_1(\lambda_C)}\right) d\lambda\right]$$

Finally:

$$\boxed{W'_\lambda = \left[1 - \varepsilon_d - \frac{e'' I_1(\lambda_C)}{\alpha I_C}\right] W_\lambda + \frac{e'' I_1(\lambda_C)}{\alpha I_C} W_1 .}$$

W_1 represents an equivalent width of the profiles of adjacent orders measured between the same columns (perpendicular to the dispersion) as W'_λ. The final expression of the measured equivalent width contains two terms: the first term depends on the exact equivalent width W_λ, while the second term depends on W_1 and should be on average close to zero.

In the first term we recognize the theoretical width diminished by scattered light in the dispersion direction (ε_d), but counterbalanced by a positive term ($-e''\ldots$) which depends on the instrumental profile.

This analytical result predicts measured equivalent widths larger than real equivalent widths, which is verified in practice.

References

Baudrand J., Catala C., 1990, Proceedings of the Second MUSICOS Workshop, Meudon, March 1990, Observatoire de Paris, p. 173

Bijaoui A., Caillat M., Pelat D., 1986, Outils pour l'analyse des images en astronomie, 2è Colloque du CESTA, ed. CESTA, Paris, p. 321

Brown T.M., Gilliland R.L., Noyes R.W., Ramsey L.W., 1991, ApJ 368, 599

Burnage R., Gerbaldi M., Proceedings of the 2nd ESO/ST-ECF Data Analysis Workshop, Garching, April 24–25, 1990, p. 137

Catala C., Foing B.H. (ed.), 1990, Proceeding of the Second MUSICOS Workshop, Meudon, March 1990, Observatoire de Paris

Cuby J.G., Baudrand J., Simon T., Proceedings of the Second MUSICOS Workshop, Meudon, March 1990, Observatoire de Paris, p. 59

Donati J.F., Semel M., Praderie F., 1989, A&A 225, 467

Felenbok P., Guérin J., 1987, Proceedings of the 132nd Symposium of the IAU, Cayrel de Strobel G., Spite M. (eds.) Paris, p. 31

Felenbok P., 1988, Comptes-rendus du Premier Atelier MUSICOS, Meudon, Juin 1988, Observatoire de Paris, p. 123

Foing B.H., Catala C., Felenbok P., 1988, Seismology of the Sun and sun-like stars, ESA SP-286, p. 665

Foing B.H., Catala C., 1991, Helioseismology from space, COSPAR XXVIII, Adv. in Space Research, Vol. 11, No. 4, p. 159

Gehren T., Ponz D., 1986, A&A 168, 386

Heacox W.D., 1986, AJ 92, 219

Hearnshaw J.B., Cottrell P.L., 1986, Instrumentation and research programmes for small telescopes, IAU, p. 371

Marechal A., 1952, Traité d'Optique Instrumentale, tome 1, ed. revue d'optique théorique et instrumentale, p. 211

McCarthy J.K., Proceedings of the 2nd ESO/ST-ECF Data Analysis Workshop, Garching, April 24–25, 1990, p. 119

Moore C.E., Minnaert M.G.I., Houtgast J., 1966, NBS, Monograph 61

Ramsey L.W., Huenemoeder P., 1986, SPIE, vol. 627, Instrumentation in Astronomy VI, p. 282

Schroeder D.J., 1967, Applied Optics 6, 1976

Schroeder D.J., 1970, A.S.P. 82, 1253

Semel M., 1989, A&A 225, 456

Spite M., Proceedings of the 2nd ESO/ST-ECF Data Analysis Workshop, Garching, April 24–25, 1990, p. 125